HOW TO TRANSPOSE A BIG MATRIX

Jon F. Claerbout

It is a lucky thing that we can easily transpose very large matrices. This is what makes wave-equation seismic data processing reasonable on a minicomputer. The transpose algorithm is simple but tricky. I shall begin, therefore, by describing a card trick. I have in my hands a deck of cards from which I have removed the nines, tens, and face cards. Let a, b, c, and d denote hearts, spades, clubs, and diamonds. Also, I have arranged these cards in the order (let ace be denoted by a one):

1a 1b 1c 1d 2a 2b 2c 2d 3a ... 8d

Now I deal the cards face up alternately, one onto pile A and one into pile B. You see

Pile A: 1a 1c 2a 2c 3a 3c ... 8a 8c
Pile B: 1b 1d 2b 2d 3b 3d ... 8b 8d

Next I place pile A on top of (in front of) pile B, and again deal the cards out alternately into pile A' and pile B'. You see

Pile A': 1a 2a 3a ... 8a 1b 2b ... 8b
Pile B': 1c 2c 3c ... 8c 1d 2d ... 8d

Now I place pile A' on top of B'. We started with all the aces together, the twos together, etc. Now we have all the hearts together, the spades together, etc. So you see that in just two deals of the cards, I have transposed the deck. We never spread the cards out all over the table because we have never had randomly to access the deck. We just made sequential passes over it. In principle, this algorithm transposes a matrix requiring four magnetic tapes but almost no core memory.

Now let us try the inverse transpose. You see that it takes me *three* deals of the cards rather than the *two* deals it took for the original transpose.

This is because the deck has $2^2 = 4$ suits and $2^3 = 8$ numbers. Actually, there is another algorithm which will allow me to do the inverse transpose in only two passes rather than three. You just do everything backwards. Start with piles A' and B'. Then create pile A by alternately selecting cards one from pile A' and one from pile B'. Likewise construct pile B. Then do it one more time. This algorithm is the "merge" algorithm.

So we see that the matrix transpose of a matrix of size $2^n \times 2^m$ can be done by the lesser of n or m passes over the data.

A variety of generalizations are possible. With 3 card piles we could work out techniques for matrices of dimension 3^n. This would decrease the number of passes but increase the required number of tape drives. Likewise it turns out that arbitrary order may be factored into primes, etc. But this takes us too far afield.

If you wish to minimize the number of passes over the data, you turn out to maximize the number of tapes. In reality you probably won't be using real tapes when you are transposing. But you are likely to be simulating tape operations on a large disk memory. Then the number of "tapes" you choose to use will be controlled by the ratio of the speed of random transfers compared to the speed of sequential transfers.

AUTOREGRESSIVE MODELLING AND SPECTRAL ESTIMATION FOR SPATIAL DATA: SOME SIMULATION EXPERIMENTS

Dag Tjøstheim

1. INTRODUCTION

Geophysical quantities often have a spatio-temporal character in the sense that they are observed both in space and in time. Examples of geophysical spatio-temporal variables are seismological array data, magnetic data, and gravity data. While a number of efficient statistical techniques exist for analysis of data recorded in time, this is not so for spatial data. In this paper we will be concerned with a new type of analysis for spatial variables. The proposed technique might be viewed as a generalization of the time-series autoregressive analysis, but there is also some justification for considering it a spatial extension of Burg's [4], [5] maximum-entropy spectral analysis (this extension problem was the original motivation for the paper).

Burg's maximum-entropy method is known to be superior to the more conventional Fast-Fourier-Transform spectral estimation method in certain situations. While the FFT technique is easily extendable from time to space, however, it turns out to be much harder to find a suitable extension of the maximum-entropy technique. Several attempts have been made to find a spatial maximum-entropy algorithm. Burg [6] has examined the problem thoroughly from a theoretical point of view, demonstrating that the "natural" spatial variational problem is extremely difficult to solve analytically. McDonough [11], [1] has presented a technique which does not derive from a fundamental variational principle, but rather from a stepwise extension of the one-dimensional method. Wernecke and D'Addario [18] study suboptimal solutions of the spatial variational problem. Their approach has the advantage of producing relatively simple numerical algorithms, which they apply on image reconstruction of astrophysical data.

For time series, it is well known [6] that the maximum-entropy variational principle results in a spectrum of so-called autoregressive type. An alternative approach, which will be pursued in this paper, therefore consists in trying to start directly from autoregressive models in space and examine their properties. This method is certainly not without difficulties, either, since the autoregressive property is a time-series concept, and it is not obvious how to generalize it to the spatial case. In fact, this problem has been studied quite extensively in the statistical literature [7], [17], [19]. In this paper, we present one particular solution of the spatial autoregressive problem. We will justify our approach in Sec. 2, where we will also have occasion to comment briefly on other models proposed. In the subsequent sections, we test various models using simulated data.

We stress at this point that the potential usefulness of autoregressive modelling is not limited to spectral analysis, but rather we look upon it as a convenient method for information compression and feature extraction of spatial data. In this context we refer to the use of one-dimensional autoregressive feature extraction as applied to waveform recognition in general [13] and to seismic discrimination in particular [16].

We will assume in this paper that the data are given on a regular grid in space. In practice this is often not the case, but methods have been proposed for getting around this problem (see [8], [14] for discussion of possible techniques and additional references). As far as estimation of spatial autoregressive coefficients is concerned, it is sufficient that the spatial *autocorrelation function* be given on a regular grid. This will become clear from Sec. 3 [see especially Eq. (3.3)].

2. THEORETICAL BACKGROUND

A p-th order autoregressive AR(p) time series $X(t)$ is defined by a p-th order difference equation

$$X(t) - a_1 X(t) - \ldots - a_p X(t - p) = Z(t) , \tag{2.1}$$

where $Z(t)$ is a white-noise time series, i.e., $E[Z(t)\, Z(s)] = \sigma_Z^2 \delta_{ts}$, and where $E[X(t)\, Z(s)] = 0$ for $s > t$. The letter E is used here to denote the statistical expectation operator. If the coefficients $a_1, \ldots, a_p$

satisfy the circle condition that $\sum_{i=1}^{n} a_i z^i = 0$ has its roots outside the unit circle in the complex z-plane, the model is said to be stable. A stable series can be written as

$$X(t) = \sum_{s=-\infty}^{t} h(t - s)\, Z(s) , \tag{2.2}$$

with the same series $Z(s)$ as in (2.1). On the other hand, a time series having the one-sided representation (2.2) can be approximated [2] by an autoregressive time series.

Let us use the notation $S\langle x,y]$ for the vectors of integers $u = (u_1,\ldots,u_n)$ which are such that $x_k \leq u_k \leq y_k$ for $k = 1,\ldots,n$, but $u \neq x$. Corresponding to (2.1) we will define an n-dimensional spatial $AR(p_1,\ldots,p_n)$ autoregressive series $F(x_1,\ldots,x_n)$ by

$$F(x) - \sum_{y \in \langle 0,p]} a(y)\, F(x-y) = Z(x) , \tag{2.3}$$

where $Z(x)$ is a spatial white-noise series such that $E[Z(y)\, F(x)] = 0$ for $y \notin S_{\_}(x)$, and where $S_{\_}(x)$ is the vectors u of integers with $u_k \leq x_k$ for $k = 1,\ldots,n$. Figure 1 illustrates the planar case. In the statistical

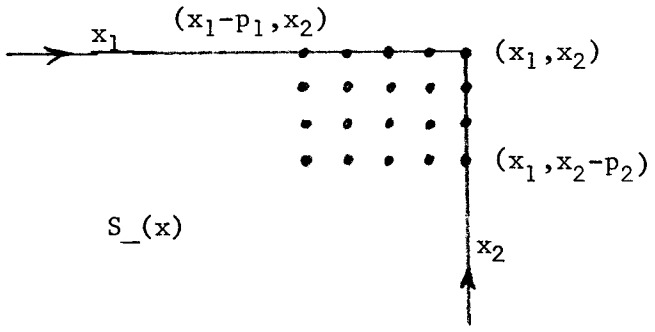

FIGURE 1.—— $S_{\_}(x)$ is the quadrant defined by the vertical and horizontal line through the point $x = (x_1,x_2)$.

literature on spatial autoregressive series, usually the models proposed have not been one-sided as in (2.3), arguing quite naturally that unlike the time-series situation, there is no preferred direction in space. This leads to difficulties, however, in the resulting statistical estimation procedures [17], [19], which is also the case when using a two-sided time-series model.

As will be demonstrated in Sec. 3, one-sided models of the form (2.3) seem to be better suited to estimation. It should also be remarked here that in some interesting recent works [9], [10] on two-dimensional system theory, the emphasis on one-sided representations analogous to (2.3) is very strong.

In the time-series case two-sided models can be reduced to one-sided models using simple transformations [19]. For multilateral spatial series an equivalent unilateral representation can be shown to *exist* (but may be difficult to obtain in practice in a general situation) under weak conditions. The problem of finding such conditions essentially reduces to the problem of finding conditions for the existence of a one-sided representation

$$F(x) = \sum_{y \in S_{-}(x)} h(x-y)\, Z(y) \tag{2.4}$$

analogous to (2.2). A spatial series having the form (2.4) can be approximated by an autoregressive series of type (2.3). Assuming the existence of a representation (2.4) is equivalent to assuming that the spectral density $f(\lambda) = f(e^{i\lambda})$ of $F(x)$ can be written as $f(e^{i\lambda}) = |\tilde{h}(e^{i\lambda})|^2$ where $\tilde{h}(e^{i\lambda})$ is the boundary-value function of a function analytic in the n-polydisc. In the one-dimensional case ($n = 1$), it is well known that a sufficient and necessary condition for this to be true is

$$\int_{-\pi}^{\pi} \log[f(e^{i\lambda})]\, d\lambda > -\infty . \tag{2.5}$$

This does not continue to hold in the spatial case, where the question of finding a necessary and sufficient condition apparently is open. However, [12, Ch. 3] a sufficient condition is that $f(e^{i\lambda})$ be positive, continuous and bounded, which is stronger than (2.5), but still a very mild condition from a practical point of view. This fact indicates that the class of spatial series that can be approximated by one-sided autoregressive series is large.

3. ESTIMATING AUTOREGRESSIVE PARAMETERS

In this section we will describe some experiments with simulated spatial autoregressive series. For the sake of simplicity we have restricted ourselves to series in the plane. A white series $Z(x_1,x_2)$ was generated using a random-number generator, and an autoregressive series $F(x_1,x_2)$ was subsequently

obtained from $Z(x_1,x_2)$ using the formula (2.3) with autoregressive coefficients $a(y_1,y_2)$ which were known to yield stability. We used the series $Z(x_1,x_2)$ as boundary values in the recursive equation (2.3) for $F(x_1,x_2)$. The task is to estimate the coefficients $a(y_1,y_2)$ from the given values $F(x_1,x_2)$.

Using the fact (see Sec. 2) that $E[Z(y)\ F(x)] = 0$ for $y \notin S_{\_}(x)$, we obtain from (2.3) a Yule-Walker type equation

$$\sum_{y \in S\langle 0,p]} R(u-y)\ a(y) = R(u), \quad \text{for} \quad u \in S\langle 0,p] \ , \tag{3.1}$$

where R is the autocorrelation function for F given by $R(x,y) = R(x-y) = E[F(x)\ F(y)]$. Suppose that we have observations of $F(x)$ for $1 \leq x_i \leq M_i$, where $M_i \geq p_i + 1$ for $i = 1,\ldots,n$. Then we can construct the following estimate $\hat{R}(u)$ of $R(u)$:

$$\hat{R}(u) = \left[\prod_{i=1}^{n} (M_i - u_i)\right]^{-1} \sum_{x \in S[1,M-u]} F(x+u)\ F(x) \ . \tag{3.2}$$

We can now obtain so-called Yule-Walker estimates of $a(y)$ by solving

$$\sum_{y \in S\langle 0,p]} \hat{R}(u-y)\ \hat{a}(y) = \hat{R}(u), \quad \text{for} \quad u \in S\langle 0,p] \ . \tag{3.3}$$

For the numerical examples in this paper, this equation was solved using direct matrix inversion. It should be noted, however, that fast algorithms (extending the one-dimensional Levinson algorithm) have been obtained. We refer again to [10]. In [15] it was shown that the estimates obtained from (3.3) are consistent; that is, the estimates $\hat{a}(y)$ converge to their true values $a(y)$ as the number of observations increases. More precisely, it was shown that a sufficient condition for the convergence of $\hat{a}(y)$ to $a(y)$ is that the product $\prod_{i=1}^{n} M_i$ tends to infinity. This result should be of some practical significance, since it means that precise estimates may be obtained even if the number of observations is increasing in one direction only. In particular, in the planar case a narrow data strip should suffice.

One of the main purposes of the simulation experiments was to look for minimal values of width and length of the data strip for which reasonable estimates are still produced. We now present the simulation results for four different models.

Theoretical Model 1: AR(1,1)

$$F(x_1,x_2) = 0.50\, F(x_1-1,x_2) + 0.33\, F(x_1,x_2-1) - 0.17\, F(x_1-1,x_2-1) + Z(x_1,x_2) \ . \tag{3.4}$$

The corresponding estimated autoregressive coefficients for various numbers of observations M_1 and M_2 in the x_1- and x_2-direction are given in Table 1. It is seen that the narrow strip consisting of 5 observations in the x_1-direction and 100 observations in the x_2-direction yields estimated values very close to the theoretical ones. Furthermore, it is seen that even with $M_1 = 5$ and $M_2 = 10$, we get reasonable results. Following [3, Ch. 8], the degree of fit can be studied empirically in terms of the estimated residual series

$$\hat{Z}(x_1,x_2) = F(x_1,x_2) - \hat{a}(1,0)\, F(x_1-1,x_2) - \hat{a}(0,1)\, F(x_1,x_2-1) - \hat{a}(1,1)\, F(x_1-1,x_2-1) \ . \tag{3.5}$$

For a perfect fit, this series should be white. The normalized residual autocorrelation function $\hat{\rho}_Z(x_1,x_2)/\hat{\rho}_Z(0,0)$ as estimated from

$$\hat{\rho}_Z(x_1,x_2) = \sum_{y_1} \sum_{y_2} \hat{Z}(x_1+y_1,x_2+y_2)\, \hat{Z}(y_1,y_2) \ , \tag{3.6}$$

is shown for a few lags x_1 and x_2 in Table 2 (with $M_1 = 5$, $M_2 = 100$). A reasonable estimate [3] of the standard error is $(M_1M_2)^{-1/2}$. It is seen that $\hat{\rho}_Z$ is roughly within a range of two standard errors, indicating that the fit is satisfactory. As could be expected, the fit deteriorates as M_2 decreases to 10.

Theoretical Model 2: AR(1,2)

$$F(x_1,x_2) = 0.67\, F(x_1-1,x_2) + 0.17\, F(x_1,x_2-1) - 0.11\, F(x_1-1,x_2-1) + 0.17\, F(x_1,x_2-2) - 0.11\, F(x_1-1,x_2-2) + Z(x_1,x_2) \ . \tag{3.7}$$

TABLE 1. Theoretical and estimated autoregressive coefficients for the AR(1,1) model defined in Eq. (3.4).

	(M_1,M_2)	$M = M_1M_2$	a(1,0)	a(0,1)	a(1,1)
Theoretical model	...	...	*0.50*	*0.33*	*-0.17*
Estimated model	(25,25)	625	0.53	0.31	-0.17
	(5,100)	500	0.51	0.34	-0.14
	(10,25)	250	0.47	0.35	-0.21
	(10,10)	100	0.53	0.19	-0.19
	(5,10)	50	0.44	0.29	-0.20
	(5,5)	25	-0.08	-0.24	0.02

TABLE 2. Estimated residual correlation function $\hat{\rho}_Z(x_1,x_2)$ for the AR(1,1) model of Table 1.

x_2 \ x_1	0	1	2	3
0	1.00	-0.01	0.00	0.09
1	-0.01	0.94	0.07	-0.03
2	0.00	0.07	0.99	-0.01
3	0.09	-0.03	-0.01	0.93

It is seen from Table 3 that the estimated model with $M_1 = 20$ and $M_2 = 20$ gives the closest approximation to the theoretical coefficients. It is interesting to note, however, that the narrow data strips $(M_1,M_2) = (8,32)$, $(8,25)$, and $(10,25)$ still appear to give reasonable approximations. This will be confirmed by spectral estimates computed in Sec. 4. To give an impression of the fit, we have estimated in Table 4 the residual process autocorrelation function for the case $M_1 = 8$ and $M_2 = 32$. Here two standard errors are given approximately by $2/\sqrt{8 \cdot 32} = 0.125$. As is seen from Table 4, the fit is satisfactory. Similar results were obtained for the other types of data strips.

Theoretical Model 3: AR(3,2)

$$\begin{aligned} F(x_1,x_2) = {} & 0.34\, F(x_1-1,x_2) + 0.64\, F(x_1-2,x_2) - 0.28\, F(x_1-3,x_2) \\ & + 0.22\, F(x_1,x_2-1) - 0.07\, F(x_1-1,x_2-1) - 0.18\, F(x_1-2,x_2-1) \\ & + 0.06\, F(x_1-3,x_2-1) + 0.36\, F(x_1,x_2-2) - 0.12\, F(x_1-1,x_2-2) \\ & - 0.23\, F(x_1-2,x_2-2) + 0.10\, F(x_1-3,x_2-2) + Z(x_1,x_2) \,. \end{aligned} \tag{3.8}$$

The corresponding estimated coefficients for various data strips are given in Table 5. Although the coefficients for $(M_1,M_2) = (4,25)$ do not look too bad, we actually had instability in this case; that is, the residual variance $\hat{\sigma}_Z^2$ was larger than the original variance $\hat{\sigma}_F^2$. We examined the fit for both $(M_1,M_2) = (20,20)$ and $(6,25)$. The autocorrelation function of the residual process indicated a considerably better fit in the case $(M_1,M_2) = (20,20)$.

Theoretical Model 4: AR(3,4)

$$\begin{aligned} F(x_1,x_2) = {} & 0.34\, F(x_1-1,x_2) + 0.64\, F(x_1-2,x_2) - 0.28\, F(x_1-3,x_2) + 0.64\, F(x_1,x_2-1) \\ & - 0.21\, F(x_1-1,x_2-1) - 0.42\, F(x_1-2,x_2-1) + 0.18\, F(x_1-3,x_2-1) \\ & + 0.44\, F(x_1,x_2-2) - 0.15\, F(x_1-1,x_2-2) - 0.26\, F(x_1-2,x_2-2) \\ & + 0.12\, F(x_1-3,x_2-2) - 0.19\, F(x_1,x_2-3) + 0.06\, F(x_1-1,x_2-3) \\ & + 0.13\, F(x_1-2,x_2-3) - 0.05\, F(x_1-3,x_2-3) - 0.06\, F(x_1,x_2-4) \\ & + 0.02\, F(x_1-1,x_2-4) + 0.04\, F(x_1-2,x_2-4) - 0.02\, F(x_1-3,x_2-4) \\ & + Z(x_1,x_2) \,. \end{aligned} \tag{3.9}$$

TABLE 3. Theoretical and estimated autoregressive coefficients for the AR(1,2) model defined in Eq. (3.7).

	(M_1,M_2)	a(1,0)	a(0,1)	a(1,1)	a(0,2)	a(1,2)
Theoretical model	...	*0.67*	*0.17*	*-0.11*	*0.17*	*-0.11*
Estimated model	(20,20)	0.71	0.15	-0.02	0.20	-0.14
	(8,32)	0.64	0.05	-0.09	0.10	-0.04
	(16,16)	0.52	0.03	-0.02	0.15	-0.06
	(10,25)	0.61	0.04	-0.11	0.12	-0.07
	(8,25)	0.63	0.03	-0.07	0.09	-0.08
	(10,10)	0.65	-0.02	-0.04	0.23	-0.29

TABLE 4. Estimated residual autocorrelation function $\hat{\rho}_Z(x_1,x_2)$ for the AR(1,2) model of Table 3.

x_2 \ x_1	0	1	2	3	4	5
0	1.00	0.06	-0.03	-0.04	0.03	0.05
1	0.06	0.94	0.03	-0.03	0.01	0.04
2	-0.03	0.03	1.01	0.06	-0.03	-0.07
3	-0.04	-0.03	0.06	0.95	0.01	-0.03
4	0.03	0.01	-0.03	0.01	1.00	0.07
5	0.05	0.04	-0.07	-0.03	0.07	0.94

From Table 6 it is seen that both of the cases $M_1 = M_2 = 25$ and $M_1 = 10$, $M_2 = 25$ give estimated models close to the theoretical model (3.9), this not being so for $M_1 = 5$, $M_2 = 25$. As for the AR(3,2) model, we found that the whitening of the residual process was significantly better for $M_1 = M_2 = 25$ than for $M_1 = 10$, $M_2 = 25$.

For this model, we also did some experiments trying to fit successively higher-order AR models to the simulated data. This was done to examine the speed of convergence of estimated coefficients to the corresponding theoretical ones. We used a data strip with $M_1 = M_2 = 25$. The results are listed in Table 7. It is seen that the lower-order model estimates are surprisingly close to the corresponding theoretical coefficients of the (3,4) model. In particular, the difference between the (3,3) and (3,4) estimated models seems to be negligible.

It is instructive in this context to look at the corresponding residual variances. As is seen from Table 8, the AR(1,2) model has a larger residual variance than the AR(2,1) model, indicating that the AR(2,1) model has the better fit of the two. This was confirmed by examining the correlation structure of the residual process. The whitening of the AR(3,3) model turned out to be excellent. This result, taken together with the fact that the residual variance for the AR(3,3) model is approximately equal to that of the AR(3,4) model shows that the series can for practical purposes be described by an AR(3,3) model.

In a practical situation when working with real data, we do not know the appropriate order for the approximating AR model, so a criterion is needed that tells us where to stop our iterative approximation procedure. In the time series case, several such criteria exist. One of the most effective is Akaike's [2] FPE criterion which consists of taking the p that minimizes the function

$$\hat{FPE}(p) = \frac{(M + p)\,\hat{\sigma}_Z^2(p)}{M - p}, \tag{3.10}$$

where $\hat{\sigma}_Z^2(p)$ is the estimated p-th order residual variance, and M is the number of observations. The appropriate spatial generalization of (3.10) can be shown to be

$$\frac{\prod_{i=1}^{n} M_i + \prod_{i=1}^{n} (p_i + 1) - 1}{\prod_{i=1}^{n} M_i - \prod_{i=1}^{n} (p_i + 1) + 1}\,\hat{\sigma}_Z^2(p_1,\ldots,p_n), \tag{3.11}$$

TABLE 5. Theoretical and estimated autoregressive coefficients for the AR(3,2) model defined in Eq. (3.8)

	(M_1,M_2)	a(1,0)	a(2,0)	a(3,0)	a(0,1)	a(1,1)	a(2,1)	a(3,1)	a(0,2)	a(1,2)	a(2,2)	a(3,2)
Theoretical model	.....	*0.34*	*0.64*	*-0.28*	*0.22*	*-0.07*	*-0.18*	*0.06*	*0.36*	*-0.12*	*-0.23*	*0.10*
Estimated model	(20,20)	0.44	0.62	-0.31	0.19	0.01	-0.21	0.09	0.34	-0.14	-0.22	0.10
	(10.25)	0.29	0.44	-0.27	0.04	-0.23	0.02	0.02	0.25	-0.07	-0.16	0.07
	(6,25)	0.42	0.57	-0.31	0.21	-0.08	-0.13	0.09	0.24	-0.21	-0.05	0.12
	(25,5)	0.13	0.57	-0.03	0.21	0.09	-0.22	-0.32	0.57	-0.13	-0.28	0.14
	(4,25)	0.53	0.74	-0.23	0.18	0.19	-0.15	0.19	0.13	0.03	-0.07	0.13
	(10,10)	0.31	0.82	-0.09	0.07	-0.40	0.04	0.11	0.43	-0.32	-0.34	0.46

TABLE 6. Theoretical and estimated autoregressive coefficients for the AR(3,4) model defined in Eq. (3,4).

	(M_1,M_2)	a(1,0)	a(2,0)	a(3,0)	a(0,1)	a(1,1)	a(2,1)	a(3,1)	a(0,2)	a(1,2)	a(2,2)	a(3,2)	a(0,3)	a(1,3)	a(2,3)	a(3,3)	a(0,4)	a(1,4)	a(2,4)	a(3,4)
Theoretical model	.....	*0.34*	*0.64*	*-0.28*	*0.64*	*-0.21*	*-0.42*	*0.18*	*0.44*	*-0.15*	*-0.26*	*0.12*	*-0.19*	*0.06*	*0.13*	*-0.05*	*-0.06*	*0.02*	*0.04*	*-0.02*
Estimated model	(25,25)	0.32	0.68	-0.27	0.61	-0.20	-0.40	0.11	0.46	-0.14	-0.30	0.20	-0.19	0.06	0.11	-0.02	-0.05	0.05	0.07	-0.06
	(10,25)	0.31	0.65	-0.30	0.49	-0.30	-0.30	0.21	0.43	-0.26	-0.26	0.24	-0.13	0.01	0.04	0.01	-0.08	0.16	-0.04	0.00
	(5,25)	0.19	0.78	-0.37	0.55	-0.12	-0.48	0.34	0.27	-0.21	-0.08	0.09	-0.01	0.01	0.15	-0.02	-0.09	0.12	-0.17	0.10

TABLE 7. Estimated lower-order autoregressive approximations of the AR(3,4) model defined in Eq. (3.9)

	Order	a(1,0)	a(2,0)	a(3,0)	a(0,1)	a(1,1)	a(2,1)	a(3,1)	a(0,2)	a(1,2)	a(2,2)	a(3,2)	a(0,3)	a(1,3)	a(2,3)	a(3,3)	a(0,4)	a(1,4)	a(2,4)	a(3,4)
Theoretical model	.....	*0.34*	*0.64*	*-0.28*	*0.64*	*-0.21*	*-0.42*	*0.18*	*0.44*	*-0.15*	*-0.26*	*0.12*	*-0.19*	*0.06*	*0.13*	*-0.05*	*-0.06*	*0.02*	*0.04*	*-0.02*
Estimated model	AR(1,1)	0.49	....	....	0.76	-0.32	....	....	....	....	....	....	....	....	....	....	....	....	....	....
	AR(2,1)	0.24	0.51	....	0.75	-0.17	-0.34	....	....	....	....	....	....	....	....	....	....	....	....	....
	AR(1,2)	0.40	....	....	0.52	-0.28	....	....	0.32	0.03	....	....	....	....	....	....	....	....	....	....
	AR(2,2)	0.18	0.55	....	0.49	-0.16	-0.23	....	0.36	0.04	-0.17	....	....	....	....	....	....	....	....	....
	AR(2,3)	0.17	0.58	....	0.58	-0.17	-0.33	....	0.45	0.01	-0.23	....	-0.19	0.05	0.11	....	....	....	....	....
	AR(3,3)	0.32	0.66	-0.28	0.61	-0.23	-0.40	0.13	0.45	-0.11	-0.28	0.17	-0.23	0.07	0.16	-0.04	....	....	....	....

TABLE 8. Residual variances for the approximating AR models of Table 7.

	Order	Variance
$\hat{\sigma}_F^2$	.....	5700
$\hat{\sigma}_Z^2$	AR(1,1)	1480
	AR(2,1)	1030
	AR(1,2)	1260
	AR(2,2)	860
	AR(2,3)	780
	AR(3,3)	720
	AR(3,4)	720

but numerical experiments are needed to test the efficiency of this criterion.

4. AUTOREGRESSIVE SPECTRAL ESTIMATION

For an autoregressive AR(p) time series as defined by (2.1), the corresponding spectral density is given by

$$f(\lambda) = \frac{\sigma_Z^2}{\left|1 - a_1\exp\{-i\lambda\} - \ldots - a_p\exp\{-ip\lambda\}\right|^2}, \tag{4.1}$$

where $-\pi \leq \lambda \leq \pi$ and where σ_Z^2 is the variance of the residual process $Z(t)$ of (2.1). Similarly for $AR(p_1,\ldots,p_n)$ spatial series of the form (2.3), it is not difficult to show that the spectral density is given by

$$f(\lambda) = \frac{\sigma_Z^2}{\left|1 - \sum_{y \in S\langle 0,p]} a(y)\ \exp\{-i[y,\lambda]\}\right|^2}, \tag{4.2}$$

where $-\pi \leq \lambda_j \leq \pi$ for $j = 1,\ldots,n$ and where $[y,\lambda] = \sum_{j=1}^{n} y_j \lambda_j$. An estimate $f(\lambda)$ of the spectral density is obtained by substituting estimates $\hat{a}(y)$ and $\hat{\sigma}_Z^2$ for the autoregressive coefficients $a(y)$ and the residual variance σ_Z^2, respectively. Hence,

$$\hat{f}(\lambda) = \frac{\hat{\sigma}_Z^2}{\left|1 - \sum_{y \in S\langle 0,p]} \hat{a}(y)\ \exp\{-i[y,\lambda]\}\right|^2}. \tag{4.3}$$

Clearly $f(-\lambda) = f(\lambda)$ and $\hat{f}(-\lambda) = \hat{f}(\lambda)$, so it suffices to do the estimation in a half-space.

Using (4.2) and (4.3), we computed the theoretical and estimated spectral density for the models 1, 2, and 3 of the preceding section for $M_1 = 10$ and $M_2 = 25$. The results are displayed in Figs. 2-4, where for matters of comparison we have also given the conventional spectral density estimate obtained using a two-dimensional FFT with subsequent smoothing. The AR estimates are seen to be much closer to the true spectra than the FFT estimates. In fact, only for model 3 does the Fourier spectrum vaguely resemble the true spectrum.

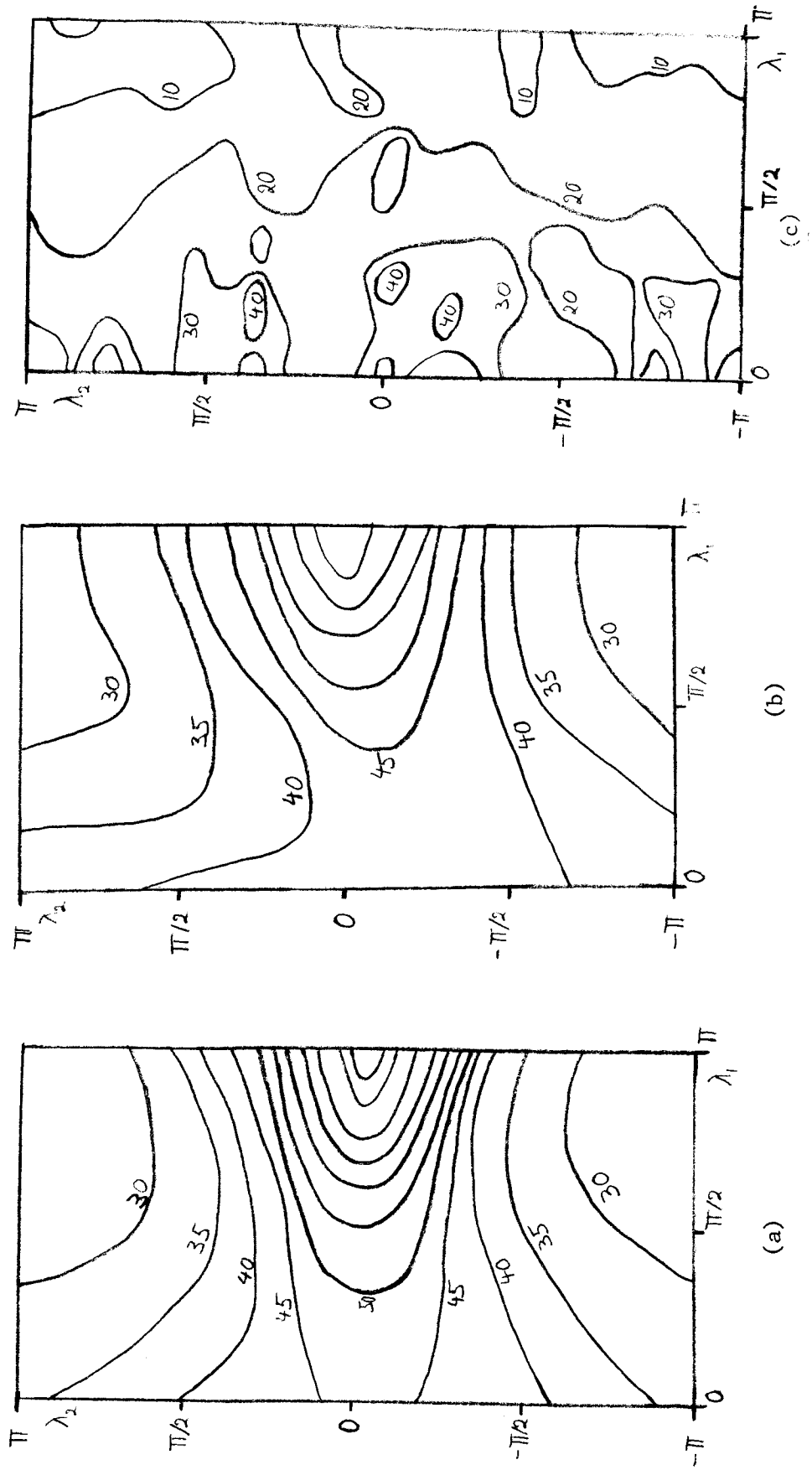

FIGURE 2.—Theoretical spectrum (a), estimated AR(1,1) spectrum (b), and estimated FFT spectrum (c) for the model defined in Eq. (3.4). Different units have been used for the FFT spectrum and the AR spectra on this figure as well as on the following figures.

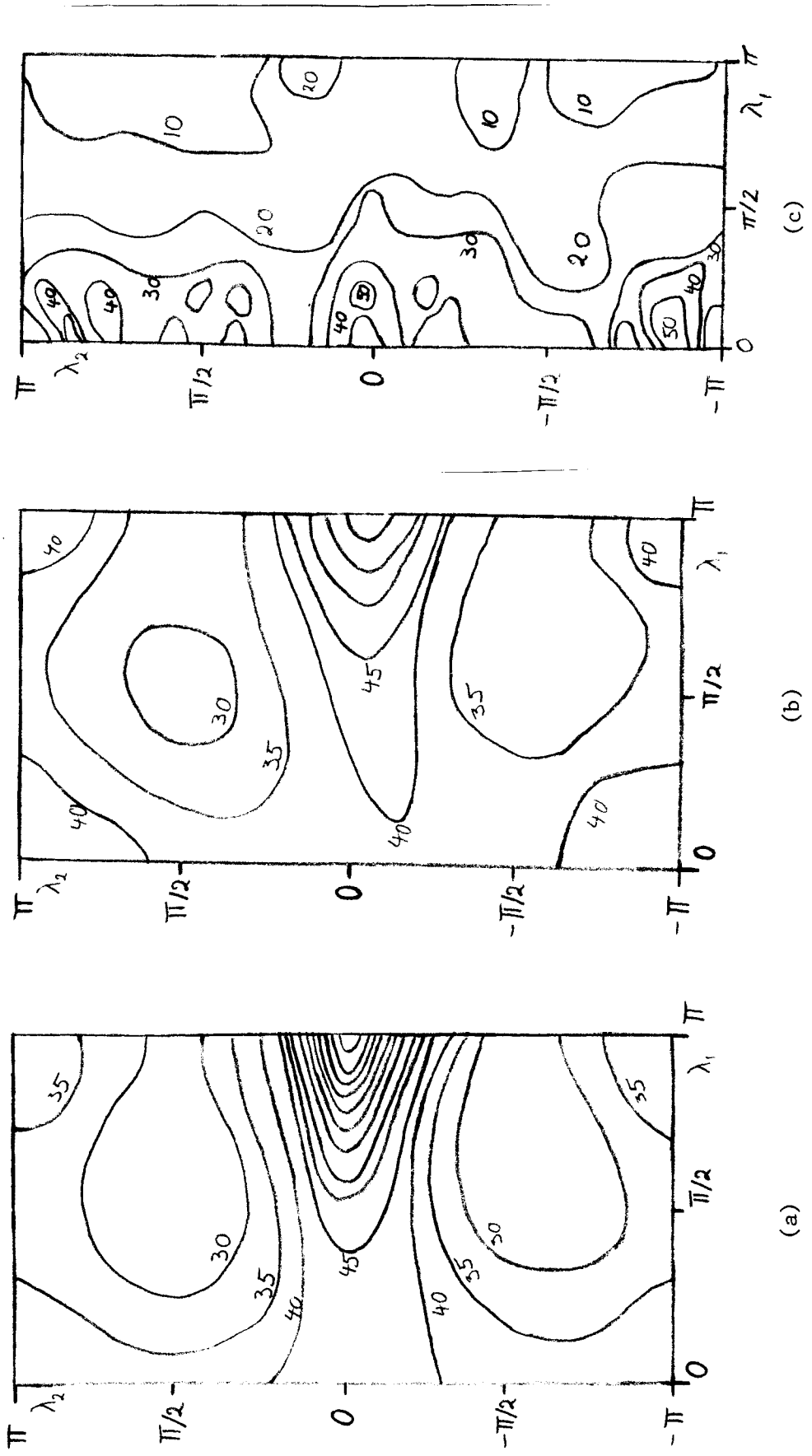

FIGURE 3.—Theoretical spectrum (a), estimated AR(1,2) spectrum (b), and estimated FFT spectrum (c) for the model defined in Eq. (3.7)

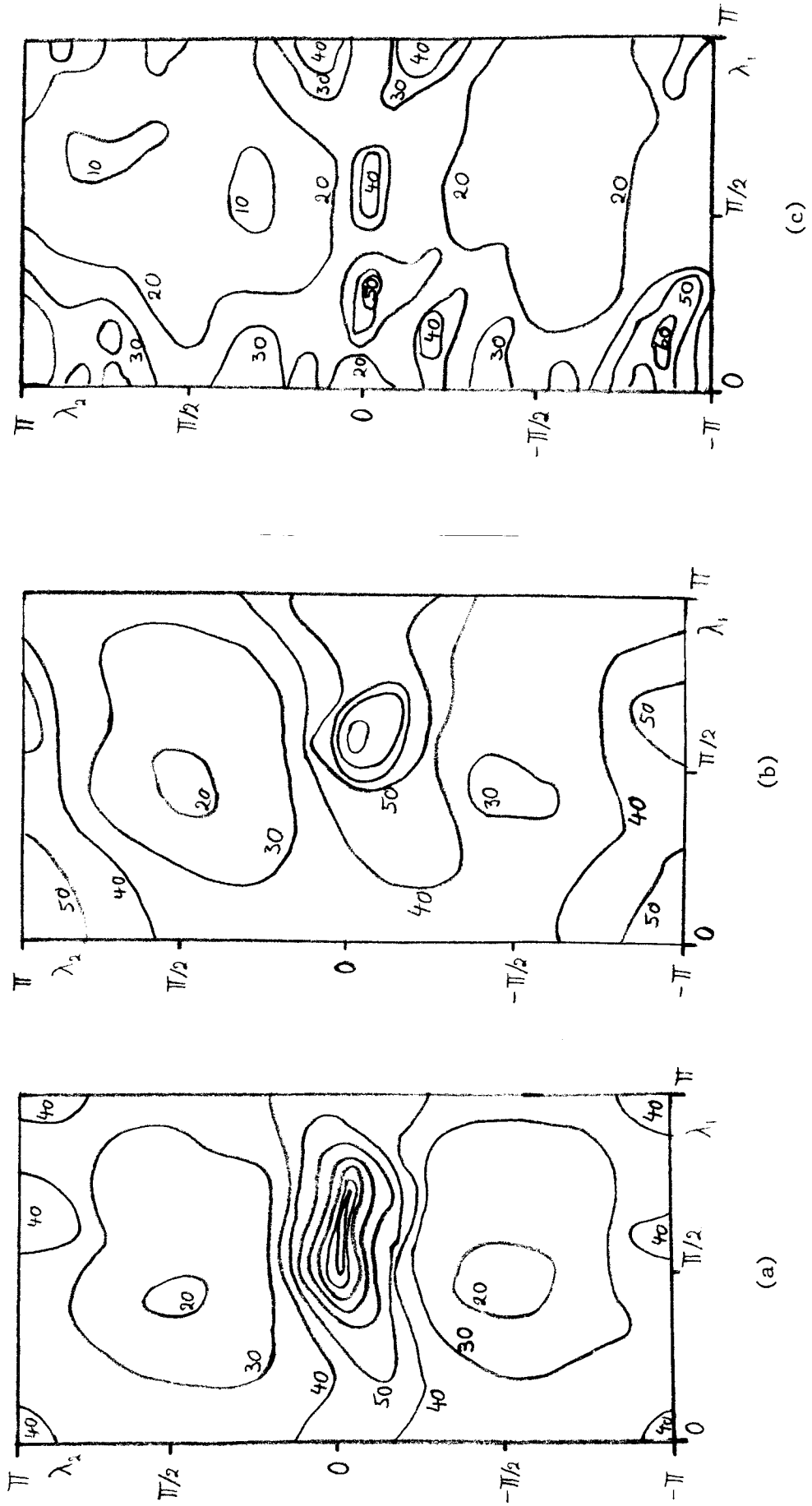

FIGURE 4.——Theoretical spectrum (a), estimated AR(3,2) spectrum (b), and estimated FFT spectrum (c) for the model defined in Eq. (3.8).

The theoretical spectra all come close to being symmetric with respect to the line $\lambda_2 = 0$. This is owing to the fact that models 1, 2, and 3 are all essentially factorizable; that is, Eq. (2.3) can be written, to a good degree of approximation, as

$$\sum_i b_i U_1^i \sum_j c_j U_2^j F(x_1,x_2) = Z(x_1,x_2) , \tag{4.4}$$

where U_i, $i = 1,2$ are the backward shift operators in the x_1- and x_2-direction, respectively. We also did tests on non-symmetric models. Thus, for the non-symmetric AR(1,1) model with theoretical coefficients 0.50, 0.33, and -0.33, we obtained estimates 0.47, 0.35, and -0.37 for $(M_1,M_2) = (10,25)$. As could be expected the resulting estimated spectrum closely resembles the theoretical spectrum. Similar results were obtained for other AR(1,1) models derived from model 1 by perturbation of the coefficients in Eq. (3.4). Clearly, more extensive testing is needed to determine the behavior of estimated coefficients and the associated spectrum in general.

As mentioned in the Introduction, autoregressive spectral estimation for time series is intimately connected with maximum-entropy spectral estimation. The spectrum of an arbitrary (possibly non-AR) time series $X(t)$ may be estimated by first fitting an AR model of sufficiently high order to the data, and then using (4.7) as an approximation to the spectral density of $X(t)$. This procedure usually works well in practice and in some situations has a resolution superior to that of the FFT estimate.

With this as our motivation, we did some simulation experiments on models of the form

$$F(x_1,x_2) = Z(x_1,x_2) + A\cos(\alpha_1 x_1 + \alpha_2 x_2) + B\cos(\beta_1 x_1 + \beta_2 x_2) , \tag{4.5}$$

where we have cosines embedded in a two-dimensional spatial white-noise series. (These models do not exhibit symmetry with respect to $\lambda_2 = 0$, of course.) Strictly speaking, such series are not covered by the autoregressive spectral estimation scheme, since the associated spectral density has singularities at $(\lambda_1,\lambda_2) = (\pm\alpha_1,\pm\alpha_2)$ and $(\lambda_1,\lambda_2) = (\pm\beta_1,\pm\beta_2)$, and hence it does not satisfy the boundedness and continuity requirement of Sec. 2.

The first experiment we did was with $A^2 \approx 0.75$ Var[Z], $B = 0$, and $(\alpha_1,\alpha_2) = (1.5,1.5)$. Again we used $M_1 = 10$ and $M_2 = 25$ observations in the

x_1- and x_2-direction, respectively. The series $F(x_1,x_2)$ was approximated successively with (2,2), (2,3), and (3,3) AR models. The results are given in Fig. 5 where an FFT estimate is displayed as well. For all four cases the spectral peak is at roughly the correct location in the λ_1-λ_2 plane. The sharpness of the peak increases substantially with the order of the approximating AR model. The (3,3) model produces a significantly sharper peak than the FFT estimate (but there are indications that a weak secondary peak may start building up for the AR estimate). Unlike Figs. 2-4 the AR-estimated contours are all more or less slanted in the same direction. We have not been able to explain exactly what causes this behavior.

It is interesting also to examine the residual variance reduction. The variance for $F(x_1,x_2)$ was 1110, while for the AR(2,2), AR(2,3), and AR(3,3) models, the residual variances were 1020, 960, and 930. The correlation structure of the residual process was not too close to that of a white-noise series, off diagonal values as high as 0.2 not being uncommon.

At the next stage both A and B of (4.5) were allowed to be non-zero. We kept (α_1,α_2) fixed at the same value as before and let $(\beta_1,\beta_2) = (0.0,1.5)$. Two values of A and B were considered: (1) $A^2 = B^2 \approx 0.75$ Var[Z] and (2) $A^2 = B^2 \approx 0.12$ Var[Z]. The corresponding estimated spectral densities are depicted in Figs. 6 and 7. For both cases the spectral peaks are slightly off their correct locations. For case (1) it is seen that the peaks are much sharper for the AR estimate than for the FFT estimate. For case (2), the presence of peaks in the FFT estimate is rather uncertain, while there still is a clear indication of two peaks for the AR estimate. They are not, however, nearly as sharp as in case (1).

Finally, we did a simulation experiment with $A^2 = B^2 \approx 0.27$ Var[Z], with $(\beta_1,\beta_2) = (0.5, 1.5)$ and (α_1,α_2) as before. As is seen from Fig. 8, the AR spectrum again gives the strongest indication of existence of the two peaks, but unfortunately the autoregressive spectral peak corresponding to $(\beta_1,\beta_2) = (0.5,1.5)$ is shifted too much to the left in the λ_1-direction. For the FFT estimate, both peaks are approximately at correct locations.

We also did some experiments with $(M_1,M_2) = (5,25)$ and with very large values for A and B. In these cases the autoregressive spectral estimates did not perform very well, possibly owing to a combined effect of a narrow data strip and a strong singularity.

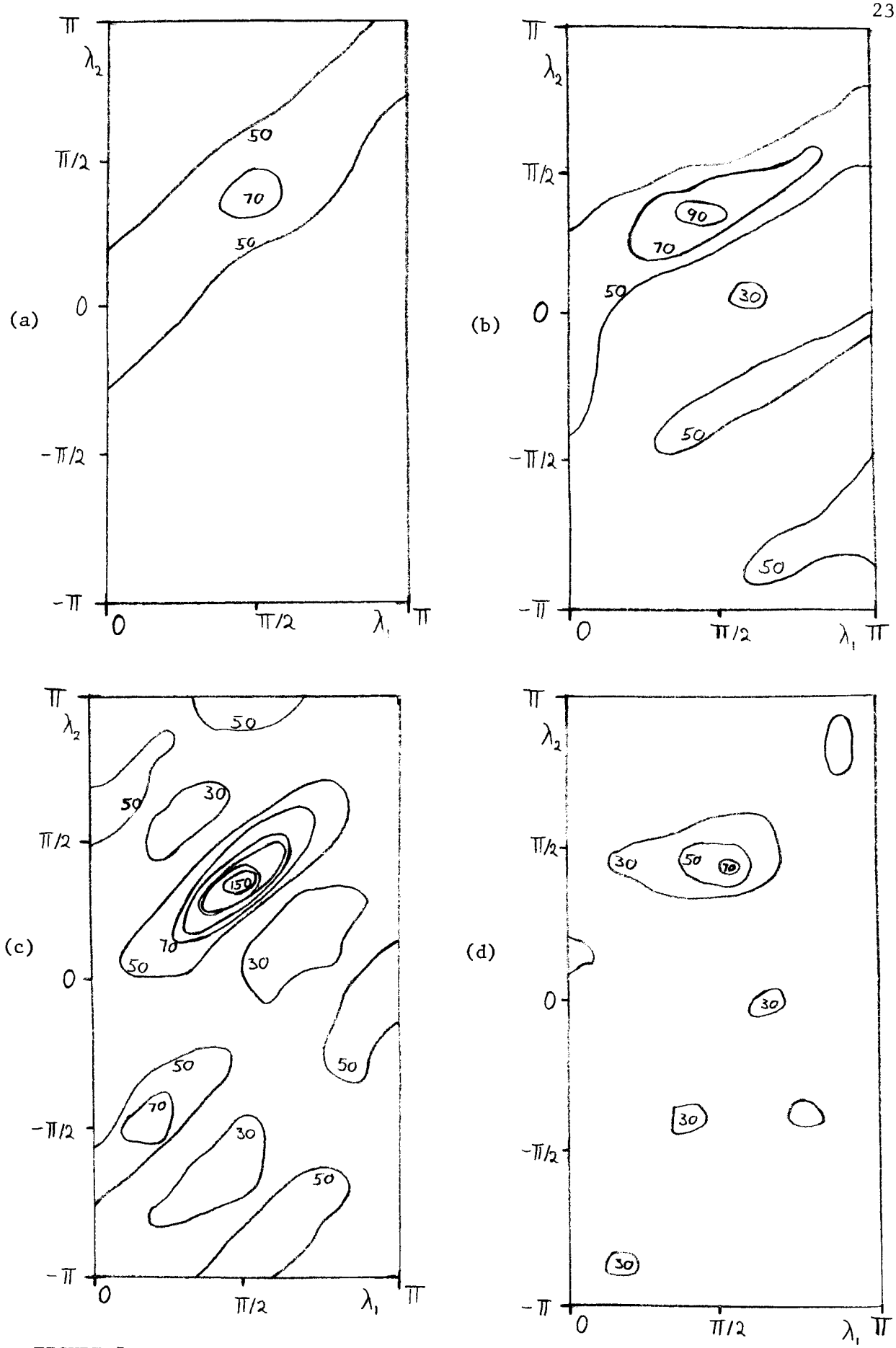

FIGURE 5.——Successive autoregressive spectral approximation (a): AR(2,2), (b): AR(2,3), (c): AR(3,3), and FFT approximation (d) of a cosine embedded in spatial white noise.

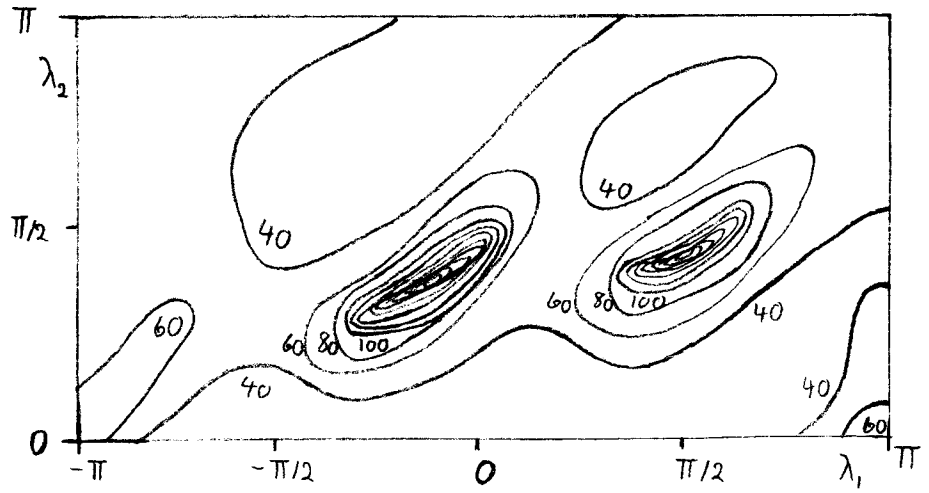

(a)

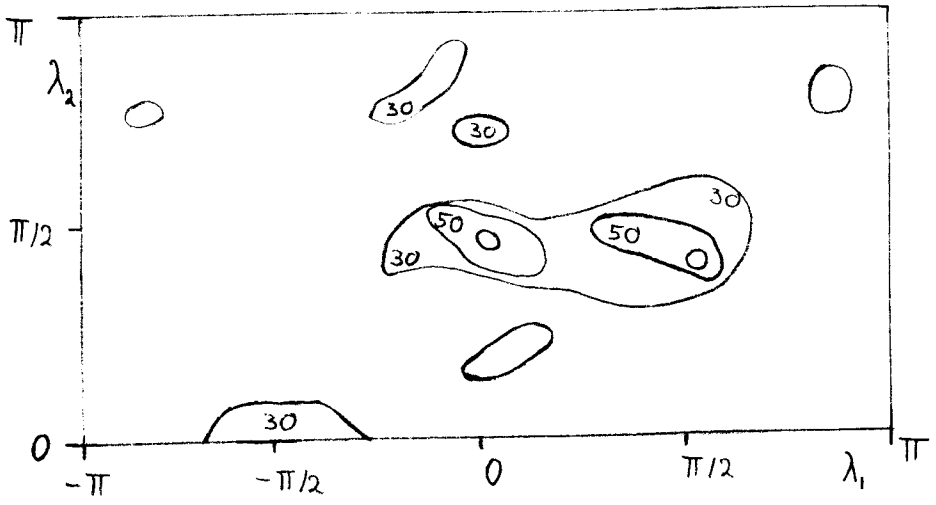

(b)

FIGURE 6.——Autoregressive AR(3,3) spectral approximation (a) and FFT approximation (b) of two high-intensity cosines embedded in white noise.

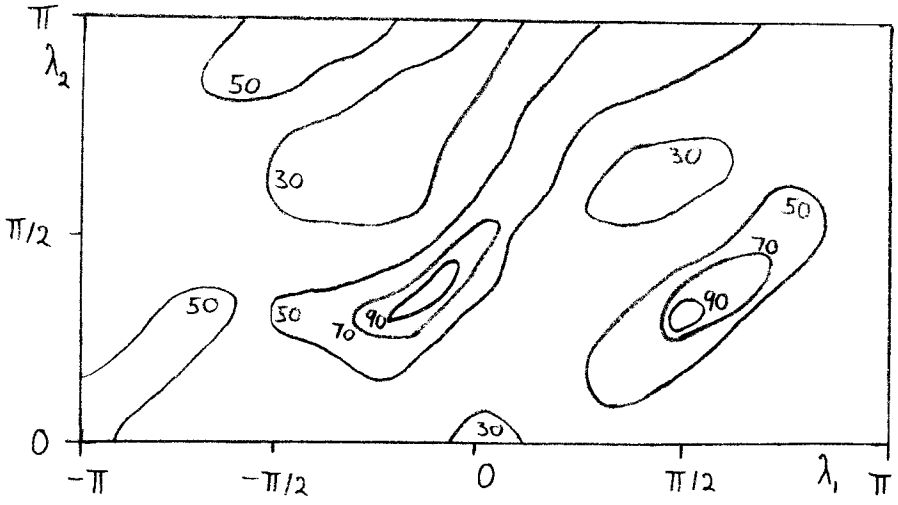

(a)

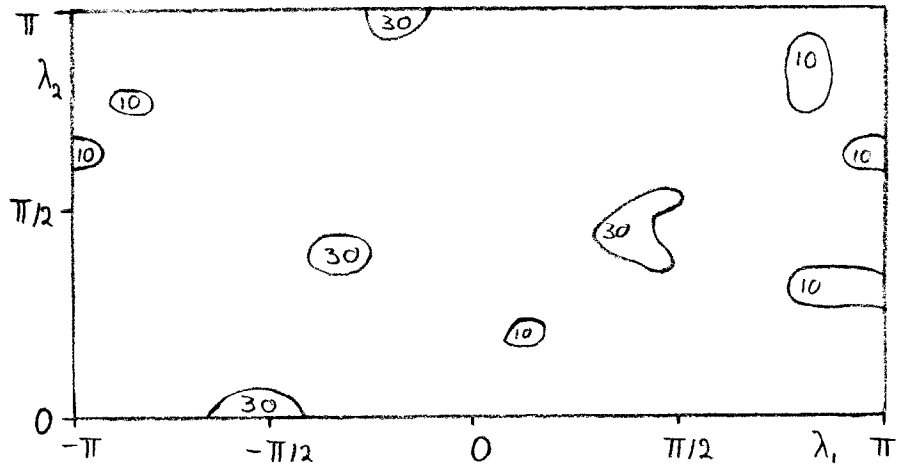

(b)

FIGURE 7.——Autoregressive AR(3,3) spectral approximation (a) and FFT approximation (b) of two low-intensity cosines embedded in white noise.

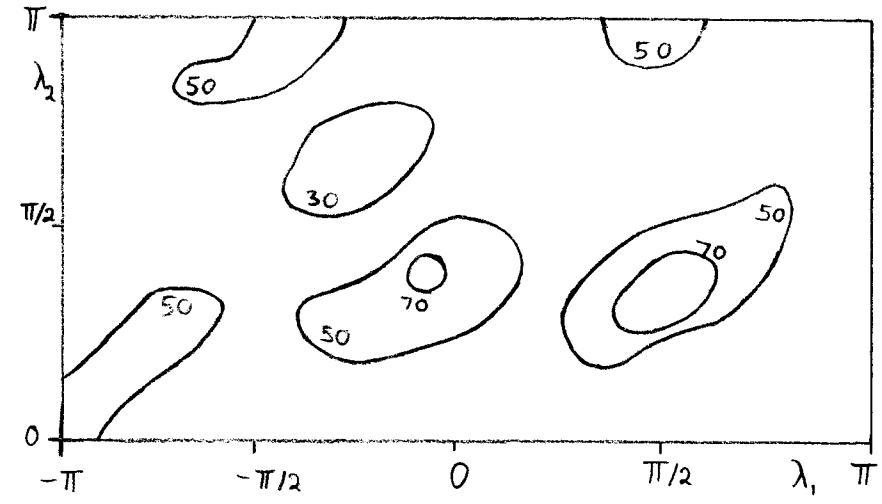

(a)

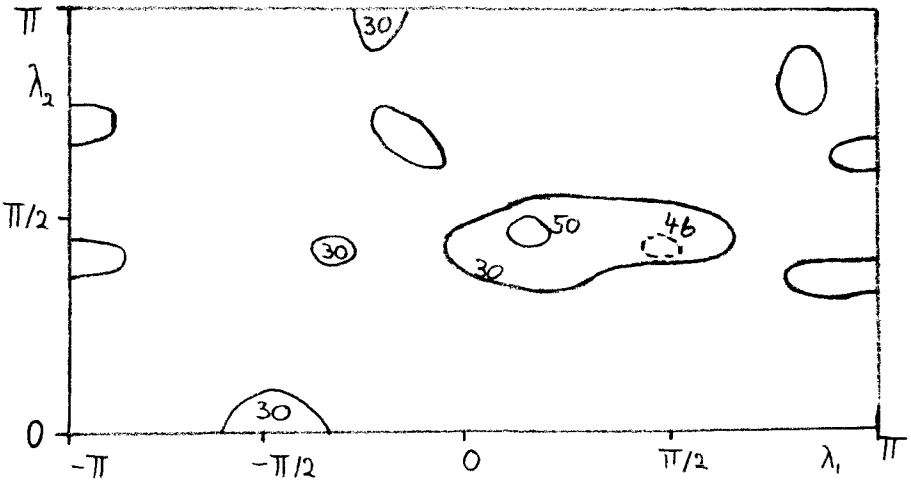

(b)

FIGURE 8.——Autoregressive AR(3,3) spectral approximation (a) and FFT approximation (b) of two cosines embedded in white noise.

From our tests we tentatively conclude that as in the time-series case, there should be situations for spatial variables where autoregressive procedures are superior to FFT estimates. More tests are required to put this conclusion on a firmer basis.

REFERENCES

[1] Adams, J.W., *Discussion* on "Maximum-entropy spatial processing of array data " by R. N. McDonough, with reply by the author, *Geophysics* 41 (1976), pp. 151-152.

[2] Akaike, H., "Statistical predictor identification," *Ann. Inst. Statist. Math.* 22 (1970), pp. 203-217.

[3] Box, G. E. P. and G. M. Jenkins, *Time Series Analysis, Forecasting and Control,* Holden Day, San Francisco, 1970.

[4] Burg, J. P., "Maximum entropy spectral analysis," presented at the 37th Meeting of the Soc. Explor. Geophys., Oklahoma City, 1967.

[5] Burg, J. P., "A new analysis technique for time series data," presented at NATO Advanced Study Inst. on Signal Processing with Emphasis on Underwater Accoustics, 1968.

[6] Burg, J. P., *Maximum Entropy Spectral Analysis,* dissertation, Depart. Geophysics, Stanford University, 1975. (Also appears as Stanford Exploration Project report SEP-8.)

[7] Cliff, A. D., and J. K. Ord, *Spatial Autocorrelation*, Pion, London, 1973.

[8] Delfiner, P. and J. P. Delhomme, "Optimum interpolation by Kriging," *NATA Advanced Study Institute on Display and Analysis of Spatial Data,* Wiley, New York, 1975, pp. 96-115.

[9] Kung, S. Y., B. Lévy, M. Morf and T. Kailath, "New results in 2-D systems theory, part II: 2D state-space models-realization and the notions of controllability, observability and minimality," *Proc. IEEE,* Special issue on Multidimensional Systems, May 1977 (to appear).

[10] Lévy, B., S. Y. Kung and M. Morf, "New results in 2D systems theory -realization and the notions of controllability, observability and and minimality," Information Systems Lab., Stanford University, 1976.

[11] McDonough, R. N., "Maximum-entropy spatial processing of array data," *Geophysics* 39 (1974), pp. 843-851.

[12] Rudin, W., *Function Theory in Polydiscs,* Benjamin, New York, 1969.

[13] Tjøstheim, D., "Recognition of waveforms using autoregressive feature extraction," *Trans. IEEE Computers*, C-26 (1977, to appear).

[14] Tjøstheim, D., "On the problem of estimating a spatio-temporal autocorrelation function," SIMS Tech. Rep., Dept. Statistics, Stanford University (1977, to appear).

[15] Tjøstheim, D., "Statistical spatial series modelling" (submitted for publication).

[16] Tjøstheim, D., and E. S. Husebye, "An improved discriminant for test ban verification using short and long period spectral parameters," *Geophys. Res. Lett.* (to appear).

[17] Unwin, D. J. and L. W. Hepple, "The statistical analysis of spatial series," *Statistician* 23 (1974), pp. 211-227.

[18] Wernecke, S. J. and L. R. D'Addario, "Maximum entropy image reconstruction," *Trans. IEEE Computers* (to appear).

[19] Whittle, P., "On stationary processes in the plane," *Biometrika* 41 (1954), pp. 434-449.